Intrinsic Fluorescence of the P-glycoprotein Multidrug Transporter: Sensitivity of Tryptophan Residues to Binding of Drugs and Nucleotides†

Ronghua Liu,‡ Aleksander Siemiarczuk,§ and Frances J. Sharom*,‡

Guelph-Waterloo Centre for Chemistry and Biochemistry, Department of Chemistry and Biochemistry, University of Guelph, Guelph, Ontario, Canada N1G 2W1, and Fast Kinetics Application Laboratory, Photon Technology International Canada Inc., 347 Consortium Court, London, Ontario, Canada N6E 2S8

Received August 9, 2000; Revised Manuscript Received September 19, 2000

ABSTRACT: P-glycoprotein is a member of the ATP binding cassette family of membrane proteins, and acts as an ATP-driven efflux pump for a diverse group of hydrophobic drugs, natural products, and peptides. The side chains of aromatic amino acids have been proposed to play an important role in recognition and binding of substrates by P-glycoprotein. Steady-state and lifetime fluorescence techniques were used to probe the environment of the 11 tryptophan residues within purified functional P-glycoprotein, and their response to binding of nucleotides and substrates. The emission spectrum of P-glycoprotein indicated that these residues are present in a relatively nonpolar environment, and time-resolved experiments showed the existence of at least two lifetimes. Quenching studies with acrylamide and iodide indicated that those tryptophan residues predominantly contributing to fluorescence emission are buried within the protein structure. Only small differences in Stern−Volmer quenching constants were noted on binding of nucleotides and drugs, arguing against large changes in tryptophan accessibility following substrate binding. P-glycoprotein fluorescence was highly quenched on binding of fluorescent nucleotides, and moderately quenched by ATP, ADP, and AMP-PNP, suggesting that the site for nucleotide binding is located relatively close to tryptophan residues. Drugs, modulators, hydrophobic peptides, and nucleotides quenched the fluorescence of P-glycoprotein in a saturable fashion, allowing estimation of dissociation constants. Many compounds exhibited biphasic quenching, suggesting the existence of multiple drug binding sites. The quenching observed for many substrates was attributable largely to resonance energy transfer, indicating that these compounds may be located close to tryptophan residues within, or adjacent to, the membrane-bound domains. Thus, the regions of P-glycoprotein involved in nucleotide and drug binding appear to be packed together compactly, which would facilitate coupling of ATP hydrolysis to drug transport.

The ABC superfamily is a large group of proteins responsible for movement of substrates across biological membranes, driven by the energy of ATP hydrolysis (*1*, *2*). The substrates moved by ABC proteins are as diverse as ions (e.g., CFTR is a chloride ion channel), and large proteins (e.g., hemolysin B exports hemolysin, an 80 kDa toxic protein). Some family members are importers, such as the bacterial histidine and maltose permeases, while others are exporters, and CFTR is a channel, rather than a transporter. The P-glycoprotein multidrug transporter (Pgp)[1] exports an astonishing variety of hydrophobic natural products, drugs, and peptides from mammalian cells, powered by the energy of ATP hydrolysis at its two nucleotide binding (NB) domains. Its physiological role is thought to involve protection against toxic xenobiotics by efflux or secretion of these compounds at the lumenal surfaces of the gut, kidney tubules, and bile ductules, and its presence in the endothelial cells of the brain appears to make a major contribution to the blood-brain barrier (*3*). Pgp also plays an important role in the multidrug resistance (MDR) displayed by many human tumors, and is an important factor in predicting the outcome of chemotherapy treatment (*4*, *5*).

The application of fluorescence techniques to the study of the structure and function of Pgp has proved very fruitful over the past few years [for reviews, see (*6*, *7*)]. Biophysical approaches such as this have been made possible by the development of methods for the isolation of sub-milligram amounts of purified Pgp with high levels of ATPase and drug transport activity. Experiments on purified Pgp labeled with the extrinsic fluorophore MIANS at Cys residues within the NB domains have led to important insights into the molecular architecture of the protein. For example, quenching experiments showed the existence of cross-talk between the

† This work was supported by a grant to F.J.S. from the National Cancer Institute of Canada (with funds provided by the Canadian Cancer Society) and the Cancer Research Society.

* To whom correspondence should be addressed at the Department of Chemistry and Biochemistry, University of Guelph, Guelph, ON, Canada N1G 2W1. Phone: 519-824-4120, Ext 2247. FAX: 519-766-1499. E-mail: sharom@chembio.uoguelph.ca.

‡ University of Guelph.

§ Photon Technology International Canada Inc.

[1] Abbreviations: AMP-PNP, 5′-adenylylimido-diphosphate; CHAPS, 3-[(3-cholamidopropyl)dimethylammonio]-1-propanesulfonate; DTE, dithioerythritol; FRET, Forster resonance energy transfer; MDR, multidrug resistance; MIANS, 2-(4′-maleimidylanilino)naphthalene-6-sulfonic acid; NATA, *N*-acetyltryptophanamide; NB, nucleotide binding; Pgp, P-glycoprotein; PMPC, palmitoylmyristoylphosphatidylcholine; TM, transmembrane; TNP-ADP/ATP, 2′(3′)-*O*-2,4,6-trinitrophenyl-adenosine-5′-diphosphate/triphosphate.

10.1021/bi0018786 CCC: $19.00
Published on Web 11/04/2000

catalytic sites in the NB domains, and the drug binding sites, which are thought to be made up by the membrane-spanning regions of the protein within the lipid bilayer (*8*). Binding to MIANS-labeled Pgp of nucleotides, and drug or peptide substrates, takes place with apparently normal affinity; however, the transporter is catalytically inactive (*8, 9*). This potential limitation can be overcome by the use of intrinsic Trp fluorescence of the catalytically active protein as a reporter technique. Trp fluorescence studies have proved invaluable for studying the interaction of a variety of ATPases and ATP-utilizing enzymes with their substrates, including the F_oF_1-ATPase (*10*), plasma membrane Ca^{2+}-ATPase (*11*), sarcoplasmic reticulum Ca^{2+}-ATPase (*12*), the DnaB helicase (*13*), and phosphofructokinase (*14*), as well as membrane transporters, such as melibiose permease (*15*) and lactose permease (*16*).

Aromatic amino acid chains, such as those of Trp, Tyr, and Phe, were found to be over-represented in the TM (transmembrane) regions of Pgp (*17*). It has been proposed that these residues, which are highly conserved across the Pgp family, may be involved in substrate recognition and interaction, and a model has been suggested whereby substrates with aromatic rings, such as rhodamine 123, can intercalate between the side chains of aromatic-rich TM helices at the protein-lipid interface (*17*). In this regard, Neyfakh and co-workers have recently proposed a working model for multidrug transporters and multidrug binding proteins, in which polyspecific recognition of multiple substrates is based on complementarity of the molecular surfaces via van der Waals interactions and overall steric fit (*18, 19*). Since many Pgp substrates contain aromatic rings, the involvement of aromatic side chains in these interactions seems likely. In addition, peptides selected from a phage display library for their ability to bind MDR drugs with high affinity were found to contain the consensus motif WXXW (*20*). Aromatic side chains such as the indole ring of Trp may thus play an important structural role in substrate recognition by Pgp, and their fluorescence properties may be sensitive to the process of substrate binding.

To date, little work has been conducted on the intrinsic fluorescence of Pgp. Sonveaux et al. reported data for quenching of the Trp fluorescence of purified Pgp with iodide ion (*21*), and, more recently, used changes in acrylamide quenching susceptibility as an indicator of conformational changes taking place on binding of various anthracycline derivatives and ATP (*22*). The fluorescence properties of the single Trp residue present within the C-terminal NB domain (NB2) of mouse Pgp were examined in a separately expressed domain, both as a fusion protein and after cleavage (*23*). Although purified NB2 was catalytically inactive, it bound fluorescent ATP and ADP derivatives, and its single Trp residue was highly quenched by binding of fluorescent nucleotides (*23*), steroids (*24*), and flavonoids (*25*).

This work reports a comprehensive study of the intrinsic fluorescence properties of purified, catalytically active Pgp in its native state. Both steady-state and lifetime experiments were used to characterize the environment of the 11 Trp residues within the protein, and the changes that take place in their fluorescence properties on substrate binding. We show that the Trp fluorescence of Pgp is highly sensitive to the binding of nucleotides, both unmodified and fluorescent derivatives, and also to the binding of a wide variety of drugs, modulators, and hydrophobic peptides that serve as substrates for the transporter. It seems likely that Trp residues are directly involved in binding of some drug substrates, and are probably in close proximity to the regions of the transporter involved in recognition of others. Our results also suggest that the site of ATP binding within the NB domains may be situated relatively close to the membrane-bound regions of the protein where many of the Trp residues are located.

MATERIALS AND METHODS

Materials. Acrylamide was obtained from Bio-Rad Laboratories (Mississauga, ON). KI was purchased from Fisher Scientific (Unionville, ON, Canada). TNP-ATP, TNP-ADP, tetramethylrosamine, and rhodamine 6G were supplied by Molecular Probes (Eugene, OR). 3-[(3-Cholamidopropyl)-dimethylammonio]-1-propanesulfonate (CHAPS), disodium-ATP, disodium-ADP, 5′-adenylylimido-diphosphate (AMP-PNP), *N*-acetyl-L-tryptophanamide (NATA), guanidine hydrochloride, colchicine, vinblastine, daunorubicin, doxorubicin, trifluoperazine, quinine, quinidine, pepstatin A, valinomycin, LY294002, rhodamine 123, and rhodamine B were purchased from Sigma Chemical Co. (St. Louis, MO). Cyclosporin A was provided by Pfizer Central Research (Groton, CT). Dr. Balázs Sarkadi (National Institute of Haematology and Immunology, Budapest, Hungary) supplied reversins 121 and 205 (*26*). PSC833 was supplied by Novartis Canada.

Purification of Pgp. Pgp was purified from the plasma membrane of MDR CH^RB30 cells by a modification of the method previously described for CH^RC5 (*27*). Following the initial extraction of plasma membrane with CHAPS buffer (25 mM CHAPS/50 mM Tris-HCl/0.15 M NaCl/5 mM $MgCl_2$/0.02% w/v NaN_3, pH 7.5), the detergent-insoluble pellet was solubilized in 15 mM CHAPS buffer, in a volume of 330 μL for each milligram of plasma membrane protein originally used. Incubation and centrifugation resulted in a soluble supernatant (S_2) which was highly enriched in Pgp. Contaminating glycoproteins were removed from the S_2 fraction by passage through a column of concanavalin A-Sepharose 4B (Pharmacia) equilibrated with 2 mM CHAPS buffer. The final product consisted of a solution of 90−95% pure Pgp, at a concentration of 0.1−0.2 mg/mL, in 2 mM CHAPS buffer. The Pgp preparation was kept on ice and used within 24 h.

Steady-State Fluorescence Measurements. Steady-state fluorescence measurements were performed using a Spex model DM3000 spectrofluorimeter (Spex Industries Inc., Edison, NJ) at 22 °C, with the excitation and emission band-pass set to 4 nm. All fluorescence studies were carried out on solutions of 100 μg/mL Pgp in 2 mM CHAPS buffer, in the presence of 0.5 mg/mL of the phospholipid palmitoylmyristoylphosphatidylcholine (PMPC; Avanti Polar Lipids, Alabaster, AL). PMPC was added as extruded 100 nm unilamellar vesicles (*8*). The excitation and emission spectra were the average of three scans, and were corrected by subtracting control scans with the same phospholipid buffer in the absence of protein.

Fluorescence Lifetime Measurements. Fluorescence decays were measured with a PTI model C-720 fluorescence lifetime instrument (*28*) (Photon Technology International Inc.,

Lawrenceville, NJ) utilizing a proprietary stroboscopic detection technique (*29*). The system employed a PTI GL-330 pulsed nitrogen laser pumping a PTI GL-302 high-resolution dye laser. The dye laser output at 590 nm was frequency-doubled to 295 nm with a GL-103 frequency doubler coupled to an MP-1 sample compartment via fiber optics. The emission was observed at 90° relative to the excitation via an M-101 emission monochromator and a stroboscopic detector equipped with a Hamamatsu 1527 photomultiplier. Fluorescence decays were analyzed with a PTI TimeMaster Pro analysis package using a discrete 1- to 4-exponential fit, 1- to 4-exponential global analysis, or lifetime distribution analysis by the Exponential Series Method (ESM) (*30*). The quality of fits was judged by chi-squared values and weighted residuals.

Quenching Studies Using Acrylamide and Iodide. Stock solutions of 5 M acrylamide, or 5 M KI, were added as 5 μL aliquots in buffer to 0.5 mL of 100 μg/mL Pgp in 2 mM CHAPS buffer with 0.5 mg/mL PMPC. All quencher solutions were freshly prepared, and 0.1 mM $Na_2S_2O_3$ was added to the KI stock solution to prevent I_3^- formation. Fluorescence emission was measured at 330 nm following excitation at 290 nm. Fluorescence intensities were corrected for dilution and scattering, and in control assays, KCl was added at the same concentration to correct for any ionic strength effects. Parallel experiments were carried out using NATA to assess quenching of Trp fluorescence by the same agents when Trp is completely accessible in aqueous solution. Quenching data were analyzed using the Stern-Volmer equation (*31*):

$$F_0/F = 1 + K_{SV}[Q]$$

where F_0 and F are the fluorescence intensities in the absence and presence of quencher, respectively, [Q] is the concentration of quenching agent, and K_{SV} is the Stern-Volmer quenching constant. In the case of a purely collisional quenching mechanism, a Stern-Volmer plot of F_0/F vs [Q] gives a linear plot with a slope of K_{SV}:

$$K_{SV} = k_q\tau_0$$

where k_q is a collisional quenching rate constant and τ_0 is the fluorescence lifetime in the absence of quencher.

Quenching Studies Using TNP-Nucleotide Derivatives and Drugs. Fluorescence quenching studies with TNP-nucleotide derivatives and various drugs and chemosensitizers were carried out on solutions of 100 μg/mL Pgp in 2 mM CHAPS buffer with 0.5 mg/mL PMPC. Working solutions of TNP derivatives and non-peptide drugs and modulators were also prepared in 2 mM CHAPS with 0.5 mg/mL PMPC vesicles, whereas peptide-based drugs and modulators were dissolved in dimethyl sulfoxide (DMSO). For the latter group of compounds, final concentrations of DMSO in the fluorescence cuvette were <10%; DMSO alone showed no effects on the Trp fluorescence of Pgp. Quenching experiments were performed by successively adding 5 μL aliquots of TNP derivatives or drug solution to 500 μL of Pgp solution in a 0.5 cm quartz cuvette. After each addition, the sample was excited at 290 nm, and the steady-state fluorescence emission was measured at 330 nm. Fluorescence intensities were corrected for dilution, scattering, and the inner filter effect as described elsewhere (*8*). Control titrations were performed with 30 μM NATA to assess the nonspecific quenching of Trp fluorescence by TNP-nucleotide derivatives and drugs.

The experimental data for nucleotides, and drugs that showed monophasic quenching behavior, were computer-fitted to the following equation, as described previously (*8*, *9*):

$$\left(\frac{\Delta F}{F_0} \times 100\right) = \frac{\left(\frac{\Delta F_{max}}{F_0} \times 100\right) \times [S]}{K_d + [S]}$$

where $(\Delta F/F_0 \times 100)$ is the percent quenching (percent change in fluorescence relative to the initial value), following addition of substrate at a concentration [S], and K_d is the dissociation constant. Fitting was carried out using nonlinear regression with the Marquardt-Levenberg algorithm (SigmaPlot, SPSS Inc., Chicago, IL), and values of K_d and $(\Delta F_{max}/F_0 \times 100)$ were extracted. For drugs that showed biphasic quenching, the experimental data were fitted to the two-site model of Doppenschmitt et al. (*32*), and two values of K_d were extracted.

Determination of the Spectral Overlap Integral. The spectral overlap integral (J) was determined using the integral equation:

$$J = \frac{\int F_D(\lambda)\epsilon_A(\lambda)\lambda^4\,\delta\lambda}{\int F_D(\lambda)\,\delta\lambda}$$

where F_D is the fluorescence intensity per unit wavelength interval in the presence of the potential donor only, ϵ_A is the molar extinction coefficient of the potential acceptor, and λ is the wavelength in centimeters. The Trp fluorescence emission spectra of Pgp was recorded using excitation at 290 nm, and the absorption spectra of TNP-nucleotide derivatives and drugs were recorded using a computer-interfaced Perkin-Elmer Lambda 6 UV/visible spectrophotometer (Perkin-Elmer, Norwalk, CT) with both sample and reference cells at 22 °C. J was calculated from the spectral data using a computer program designed solely for that purpose by Dr. Uwe Oehler (Department of Chemistry and Biochemistry, University of Guelph).

The quantum yield of Pgp Trp fluorescence, Q, was determined relative to NATA as a standard. Both the sample and standard had the same absorbance value of 0.095 at 290 nm. The quantum yield of Pgp was calculated using the equation:

$$Q_{Pgp} = \frac{F_{Pgp}}{F_{NATA}} \times Q_{NATA}$$

where Q_{NATA}, the quantum yield of NATA, is known to be 0.14 (*33*), and F_{Pgp} and F_{NATA} are the integrals of the fluorescence emission of Pgp and NATA in the wavelength range 310−500 nm.

RESULTS

Location of Trp Residues within Hamster Pgp. Hamster Pgp [the Pgp1 gene product (*34*)] contains 11 Trp residues distributed throughout the protein. The schematic diagram shown in Figure 1 displays the placement of these Trp

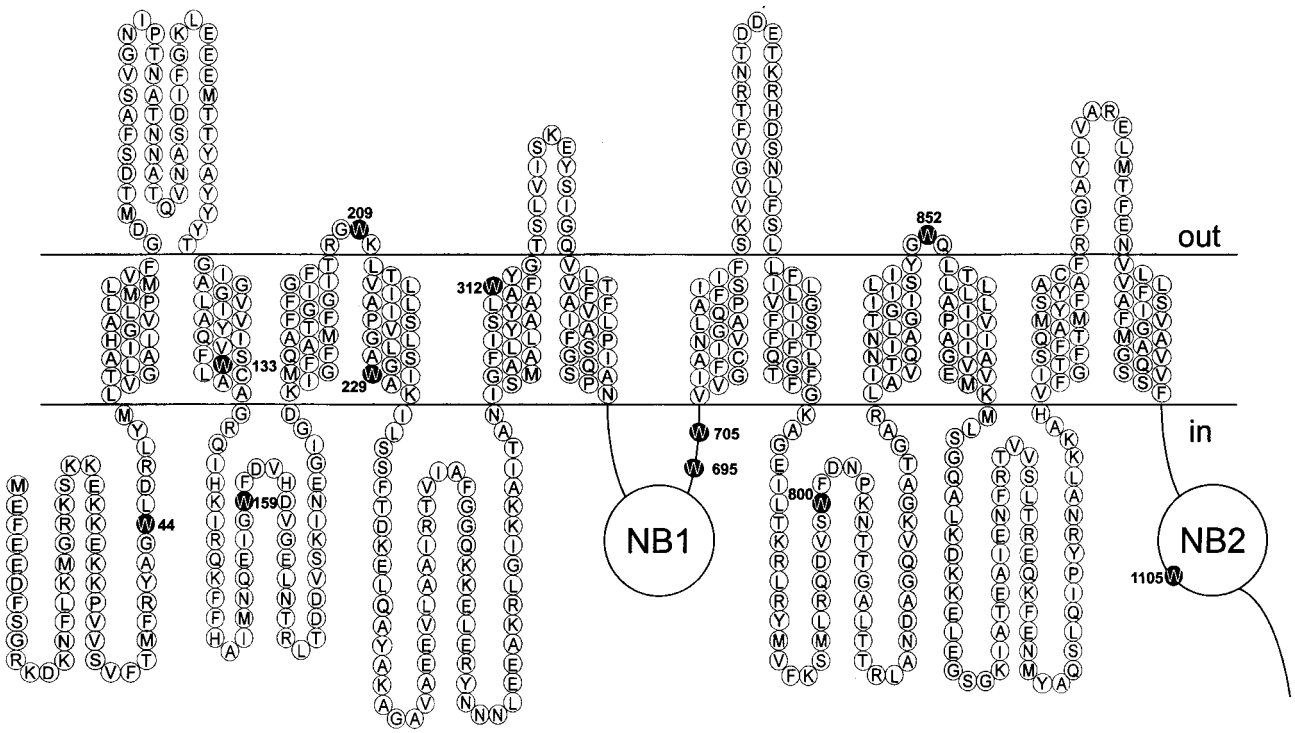

FIGURE 1: Schematic diagram showing the location of the 11 Trp residues within the hamster class I Pgp, based on a topology model similar to that proposed for the murine mdr3 protein (*35*). The N-half of the transporter contains 8 Trp residues: Trp44 in the N-terminal tail; Trp133, Trp229, and Trp312 in TM2, TM4, and TM5, respectively; Trp159 in the first cytoplasmic loop; Trp209 in the second extracellular loop; and Trp695 and Trp705 in the linker region immediately following NB1. The C-half of Pgp contains 3 Trp residues: Trp800 in cytoplasmic loop 3, Trp852 in extracellular loop5, and Trp1105 between the Walker A and B motifs of NB2.

residues within hamster Pgp1, based on the proposed topology for the mouse mdr3 homologue (*35*). The N-terminal half of Pgp contains seven Trps, and the C-terminal half contains four residues. Three residues in the N-half (Trp133, Trp229, and Trp312) are located within putative TM segments 2, 4, and 5, respectively. Trp44 is positioned in the N-terminal tail, and Trp159 and Trp209 in an intracellular and extracellular loop, respectively. Two residues (Trp695 and Trp705) are found in the linker region following NB1, just upstream of TM7. In the C-half, residues 800 and 852 are located in an intracellular and extracellular loop, respectively, and Trp1105 is situated within NB2, between the Walker A and B motifs. The position of these Trp residues is highly conserved in both the human (MDR1) and mouse (mdr3) homologue.

Characterization of the Intrinsic Trp Fluorescence of Purified Pgp. Purified, catalytically active Pgp was isolated from MDR CH^{R}B30 Chinese hamster ovary cells. Steady-state and lifetime fluorescence studies were carried out in order to characterize the properties and environment of the Trp residues. All measurements were carried out in the presence of the phospholipid PMPC, which gave the lowest background fluorescence of several lipids tested under the experimental conditions. Pgp has previously been successfully reconstituted into proteoliposomes of PMPC in the fully active form (*36*). The presence of phospholipids was necessary to observe reproducible high-level quenching of Trp fluorescence induced by substrate binding (see below). The emission spectrum of purified Pgp ($\lambda_{ex} = 290$ nm) exhibited a maximum at 333 nm, indicating that the Trp residues of Pgp are located in a highly nonpolar environment compared to the soluble Trp analogue, NATA, which displayed an emission maximum at 356 nm (Figure 2). Pgp underwent a large red shift (14 nm) in fluorescence emission to 347 nm following denaturation of the protein in 6 M guanidine hydrochloride (Figure 2), which would largely unfold the protein. Several of the Trp residues in Pgp are located in extramembranous regions of the protein and are thus potentially highly accessible to their aqueous surroundings. The relatively hydrophobic environment indicated by the emission maximum suggests either that these residues do not contribute to the observed fluorescence emission (i.e., they are internally quenched), or that they are present in nonpolar regions within tightly folded protein domains.

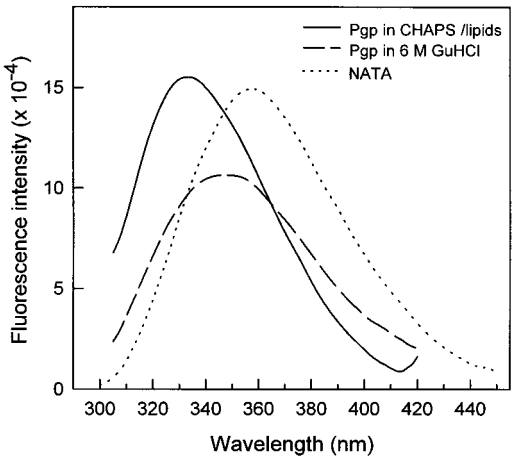

FIGURE 2: Corrected fluorescence emission spectra for purified native Pgp (100 μg/mL) in buffer containing 2 mM CHAPS and 0.5 mg/mL PMPC (——), and following treatment with 6 M guanidine hydrochloride (GuHCl; - - -), compared with 30 μg/mL of the soluble Trp analogue NATA (•••). Fluorescence emission was recorded at 22 °C following excitation at 290 nm.

Table 1: Acrylamide Quenching Effect on Pgp Trp and NATA Fluorescence Lifetimes

sample[a]	α_1	τ_1 (ns)	α_2	τ_2 (ns)	α_1/α_2	$\langle\tau_{av}\rangle$ (ns)
Pgp alone	0.276	0.64	0.314	4.0	0.879	2.43
Pgp + acrylamide						
0.098 M	0.302	0.64	0.210	4.0	1.43	2.02
0.192 M	0.215	0.64	0.136	4.0	1.58	1.94
0.283 M	0.270	0.64	0.149	4.0	1.81	1.83
0.370 M	0.194	0.64	0.0921	4.0	2.11	1.72
0.455 M	0.184	0.64	0.0938	4.0	1.96	1.78

sample[b]	α_1	τ_1 (ns)	τ/τ_0
NATA alone	0.949	2.63	1.00
NATA + acrylamide			
0.098 M	0.680	1.03	0.392
0.192 M	0.456	0.616	0.234
0.283 M	0.302	0.497	0.189
0.370 M	0.245	0.351	0.133

[a] Two-exponential global analysis was carried out, using the same two lifetimes of 0.64 and 4.0 ns for all decays. α is the preexponential value; τ is the fluorescence lifetime; $\langle\tau_{av}\rangle$ is the amplitude average lifetime. [b] Decays were fitted to a single-exponential function.

Fluorescence Lifetime of Trp Residues in Pgp. The fluorescence decay of NATA could be adequately described by a single-exponential function with a lifetime, τ, of 2.6 ns (Table 1). However, as shown in Figure 3A, two exponentials were required to obtain a satisfactory fit for the Pgp Trp decay. The longer lifetime component of ~4 ns made the major contribution to the overall fluorescence compared to the shorter component, which had a lifetime of 0.6−1 ns (range observed for several different Pgp preparations). As Pgp contains 11 Trp residues distributed over different domains, the decay complexity is not surprising, and in fact, one may even expect a distribution of fluorescence lifetimes. Therefore, the Pgp fluorescence decay depicted in Figure 3A was also analyzed in terms of a lifetime distribution with the Exponential Series Method (ESM) (*30*). This analysis resulted in a bimodal distribution with the average lifetime values of 0.73 and 4.2 ns (Figure 3B), thus being very close to the values recovered from the discrete double exponential fit. The amplitude-weighted average lifetime for Pgp was calculated as 2.4 ns.

Quenching of Trp Residues by Acrylamide and Iodide. Acrylamide is an excellent neutral quencher that is sensitive to exposure of Trp residues in proteins. Quenching of the Trp fluorescence of Pgp was measured over the range of 0−0.5 M, and compared to that of the soluble Trp analogue, NATA (Figure 4A,B). ATPase assays showed that acrylamide had little effect on the hydrolysis of ATP by Pgp up to a concentration of 0.3 M, with only a small decline in the catalytic activity of ~20% taking place over the range 0.3−0.5 M (data not shown). Thus, even relatively high concentrations of the quencher are expected to have only limited effects on Pgp conformation. The linear Stern-Volmer plot (an expanded plot is shown in Figure 4B) suggests that only a single class of Trps within Pgp is quenched, and they are all equally accessible to quencher. Slight shifts in the emission maximum were noted as the concentration of acrylamide increased up to 0.3 M, possibly related to the small loss of enzymatic activity noted above. The slope of the Stern-Volmer plot for Pgp was 2.61 ± 0.022 M^{-1}, compared to 23.1 ± 0.35 M^{-1} for NATA; the ~9-fold lower value indicates that the Trp residues contributing to fluorescence emission in the transporter are largely buried. Assuming that quenching was governed by a collisional mechanism, we calculated the biomolecular quenching constant, k_q, which is a measure of the intrinsic susceptibility of the Trp residues of Pgp to collisional quenching by acrylamide. The value of 1.1×10^9 M^{-1} s^{-1}, compared to that of 8.8×10^9 M^{-1} s^{-1} for NATA, again indicates that the Trp residues in Pgp are relatively inaccessible. NATA fluorescence is not affected by addition of PMPC vesicles, confirming that aqueous quenching is being measured in that case. Pgp in detergent solution also showed no difference in quenching from protein in the presence of phospholipid, so it does not appear that the lipid bilayer "shields" the protein from contact with acrylamide. Thus, it seems likely that protein conformation and folding determine accessibility to this quencher.

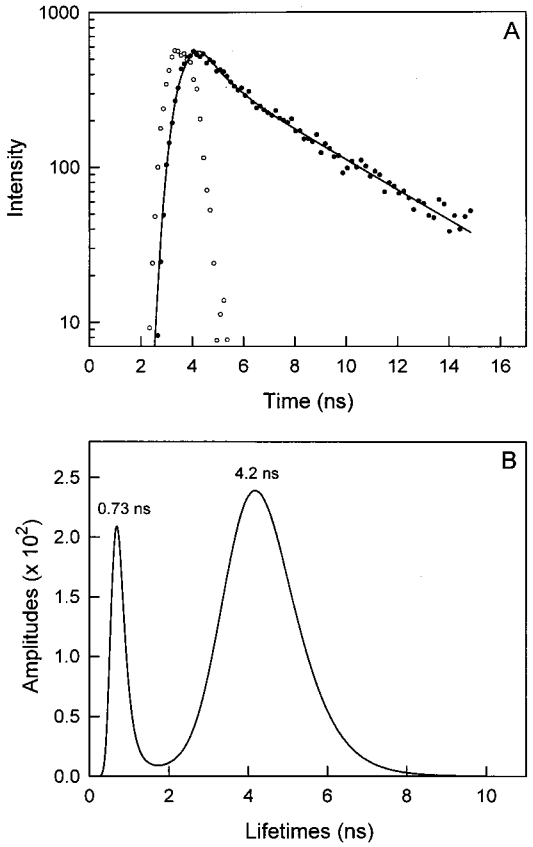

FIGURE 3: (A) Fluorescence decay of purified Pgp in buffer containing 2 mM CHAPS and 0.5 mg/mL PMPC. Fluorescence emission was collected at 350 nm following excitation at 295 nm. Double exponential analysis recovered the following values: $\alpha_1 = 0.32$, $\tau_1 = 0.68$ ns, $\alpha_2 = 0.28$, $\tau_2 = 4.2$ ns, $\alpha_1/\alpha_2 = 1.1$, $\chi^2 = 1.08$. (B) Lifetime distribution analysis with ESM of the Pgp decay shown in (A). Lifetime values averaged over respective peaks are 0.73 and 4.2 ns, the ratio of integrated amplitudes $\alpha_1/\alpha_2 = 1.0$, and $\chi^2 = 1.07$.

Preliminary double-exponential decay analysis showed no trend for individual Pgp Trp residues as a function of acrylamide concentration. The set of decay curves was thus analyzed with the double-exponential global analysis program, where the individual lifetime components were constrained to be the same for all decay files, and only preexponential factors were free-floating (Table 1). The average lifetime, $\langle\tau_{av}\rangle$, decreased with increasing acrylamide concentration, but not in proportion to the decrease in fluorescence intensity, as expected for purely collisional

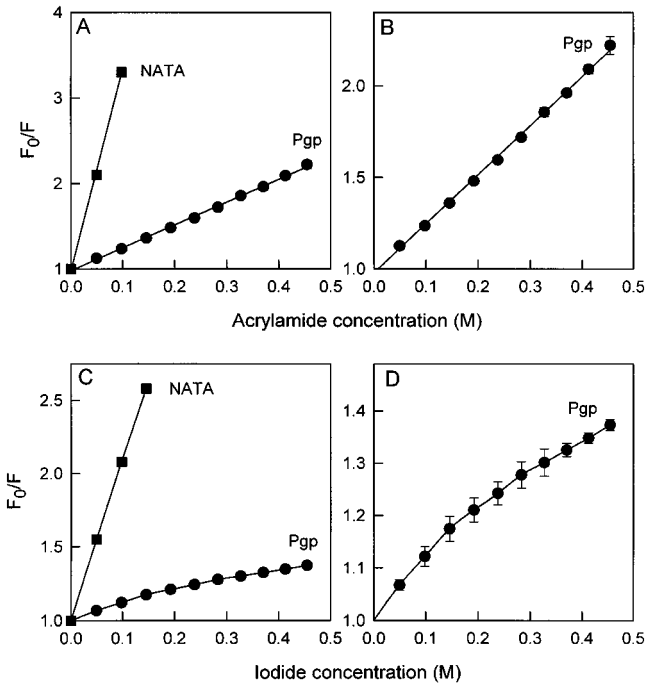

FIGURE 4: Stern-Volmer plots for quenching of the intrinsic Trp fluorescence of Pgp by acrylamide (A, B) and I^- (C, D). Expanded plots for Pgp quenching are shown in (B) for acrylamide and in (D) for I^-. Aliquots of the appropriate quencher were added to a 100 μg/mL solution of purified Pgp in buffer containing 2 mM CHAPS and 0.5 mg/mL PMPC. Parallel experiments were carried out with 30 μg/mL NATA. Fluorescence emission at 330 nm was recorded at 22 °C following excitation at 290 nm. Where not visible, error bars are contained within the symbols.

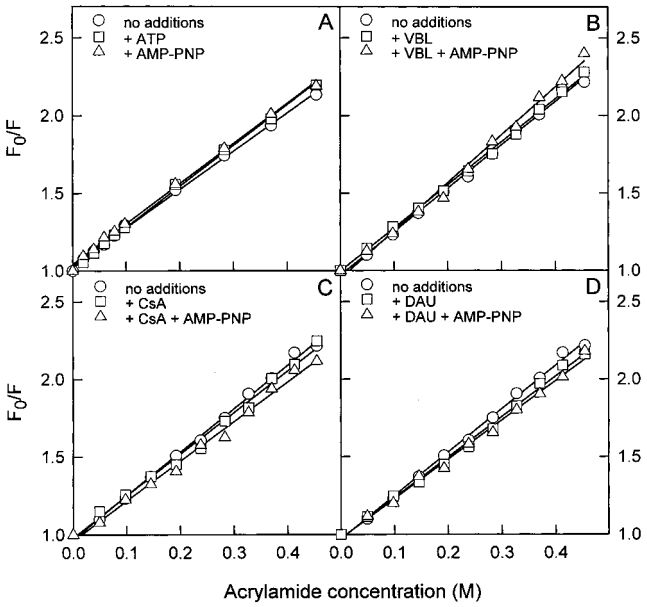

FIGURE 5: Acrylamide quenching of the intrinsic Trp fluorescence of Pgp in the presence of various nucleotides and drug substrates. Aliquots (5 μL) of a 5 M solution of acrylamide were added at 22 °C to 0.5 mL of a 100 μg/mL solution of purified Pgp in buffer containing 2 mM CHAPS and 0.5 mg/mL PMPC. (A) Pgp alone (○), and in the presence of 2 mM ATP (□) or 2 mM AMP-PNP (△). (B) Pgp alone (○), or in the presence of 10 μM vinblastine (VBL, □) or 10 μM vinblastine + 2 mM AMP-PNP (△). (C) Pgp alone (○), or in the presence of 10 μM cyclosporin A (CsA, □) or 10 μM cyclosporin A + 2 mM AMP-PNP (△). (D) Pgp alone (○), or in the presence of 20 μM daunorubicin (DAU, □) or 10 μM daunorubicin + 2 mM AMP-PNP (△). Fluorescence emission at 330 nm was recorded at 22 °C following excitation at 290 nm. Where not visible, error bars are contained within the symbols.

quenching. The values of α_1 and α_2 (which are expected to be independent of [Q]) both decreased, and the ratio of preexponential factors (α_1/α_2) recovered from the global analysis also increased dramatically, suggestive of a strong static quenching component. In contrast, NATA showed a large decrease in the fluorescence lifetime with increasing acrylamide concentrations (Table 1). The Stern-Volmer quenching constant for NATA calculated from the lifetime data was 17.0 M^{-1}, indicating that dynamic quenching is the major mechanism accounting for the observed decrease in the steady-state fluorescence for NATA. However, the preexponential factor is also affected, suggesting that static quenching makes an additional contribution (Table 1).

Additional information on Trp location can be provided by quenching with ionic species. Heavy atoms such as I^- cannot penetrate the nonpolar interior of proteins, and selectively quench only surface Trp residues. I^- was a very poor quencher of Trp residues within Pgp compared to NATA (Figure 4C,D). The quenching plot (shown in expanded form in Figure 4D) was nonlinear with a downward curve, suggesting that two classes of Trp residues exist, one of which is highly inaccessible to I^-. The K_{SV} value for I^- quenching of NATA was 10.9 ± 0.053 M^{-1}, ~8.5−13-fold higher than the slope of the plot for Pgp over the concentration range 0−0.5 M (0.84 ± 0.020 to 1.27 ± 0.033 M^{-1}). These results indicate that there are two classes of Trp residues, both largely buried, within either the membrane or the protein structure.

Acrylamide Quenching in the Presence of Nucleotides and Drug Substrates. Acrylamide quenching of Trp residues was carried out in the presence of saturating concentrations of nucleotides (both hydrolyzable and nonhydrolyzable), various drug substrates, and combinations of the two. Significant conformational changes arising from substrate binding would be expected to result in altered Trp accessibility, and changes in susceptibility to acrylamide quenching. As shown in Figure 5A, addition of saturating concentrations of either ATP or the nonhydrolyzable analogue AMP-PNP resulted in only very small changes in the slope of the Stern-Volmer plot, indicating a slight increase in accessibility of Trp residues to solvent. Addition of vinblastine gave a similarly small increase in slope, which was increased further by the addition of AMP-PNP (Figure 5B). Cyclosporin A (Figure 5C) and daunorubicin (Figure 5D) also showed small changes in the slope of the plots, but in the opposite direction, with addition of drug resulting in reduced accessibility of Trp residues to solvent, and addition of AMP-PNP causing a further reduction. These results suggest that any conformational changes taking place on binding of drugs and nucleotides have only small effects on the solvent accessibility of Pgp Trp residues.

Quenching of Trp Residues by Nucleotide Binding. Binding of substrates to proteins can often cause quenching of the intrinsic Trp fluorescence. Addition of ATP (Figure 6A) and ADP (data not shown) to Pgp resulted in saturable, concentration-dependent quenching of Trp fluorescence. Fitting of the quenching data to an equation representing interaction with a single type of binding site resulted in the estimation of two parameters: the dissociation constant for binding, K_d, and the maximal quenching reached at saturation, ΔF_{max}. Values of K_d for ATP and ADP were around 0.3 mM (Table 2), which is almost identical to the values of K_d estimated

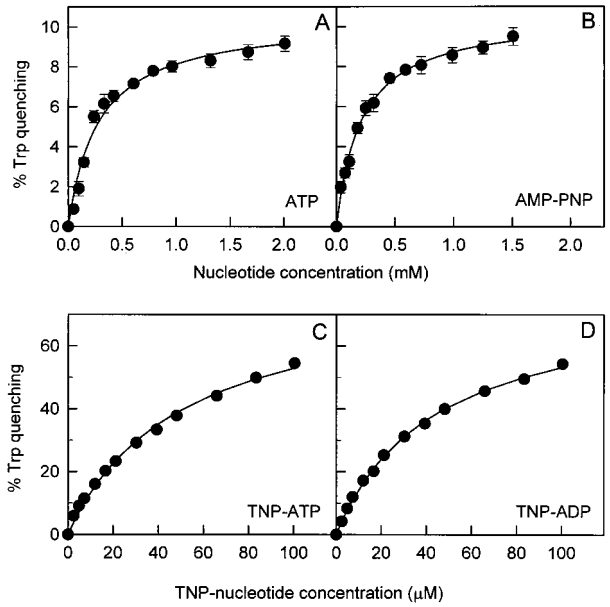

FIGURE 6: Effect of nucleotide binding on the intrinsic Trp fluorescence of Pgp. Increasing concentrations of (A) ATP, (B) AMP-PNP, (C) TNP-ATP, and (D) TNP-ADP were added at 22 °C to a 100 μg/mL solution of purified Pgp in buffer containing 2 mM CHAPS and 0.5 mg/mL PMPC. Fluorescence emission at 330 nm was recorded at 22 °C following excitation at 290 nm. Where not visible, error bars are contained within the symbols.

Table 2: Binding Parameters for Quenching of Pgp Trp Fluorescence by Nucleotides, and Drug and Peptide Substrates

substrate	K_{d1} (μM)[a]	K_{d2} (μM)[a]	ΔF_{max1} (%)[b]	ΔF_{max2} (%)[b]	total ΔF_{max}[c]
nucleotides					
ATP	280		10.4		10.4
ADP	330		9.46		9.46
AMP-PNP	210		10.6		10.6
TNP-ADP	43.9		76.5		76.5
TNP-ATP	50.6		79.6		79.6
non-peptide drugs					
colchicine	74.9		102		102
quinine	12.5		33.5		33.5
quinidine	7.76		18.5		18.5
rhodamine 123	1.88	29.3	19.3	67.8	87.1
doxorubicin	1.72	20.5	9.66	18.9	28.6
LY294002	1.55	30.2	13.8	28.1	41.9
daunorubicin	1.42	42.3	13.6	40.9	54.5
rhodamine B	1.23	62.9	6.58	118	125
trifluoperazine	0.89	9.39	14.1	22.7	36.8
vinblastine	0.50		17.5		17.5
rhodamine 6G	0.46	6.46	21.3	7.3	28.6
tetramethylrosamine	0.25	14.9	6.29	55.5	61.8
peptides and peptide-based drugs					
pepstatin A	9.53		4.46		4.46
valinomycin	0.72		4.14		4.14
reversin 205	0.37		5.41		5.41
cyclosporin A	0.30		4.44		4.44
reversin 201	0.23		6.18		6.18
PSC833	0.081		4.02		4.02

[a] Dissociation constants for binding were obtained by fitting of the Trp quenching data to an equation for either a single binding site (K_{d1}) or (where appropriate) two binding sites, one of high affinity (K_{d1}) and one of lower affinity (K_{d2}) (*32*). [b] ΔF_{max} values were also obtained from fitting of the quenching data. Where a clearly biphasic quenching curve was observed, a two-site model was used, and the values for both the higher (ΔF_{max1}) and the lower affinity (ΔF_{max2}) binding component are shown. [c] The total ΔF_{max} is the sum of ΔF_{max1} and ΔF_{max2}.

from quenching of MIANS-labeled Pgp (*8*), and very similar to the K_M for ATP hydrolysis (*27*). Thus, Trp residues within Pgp are sensitive to nucleotide binding, and quenching data

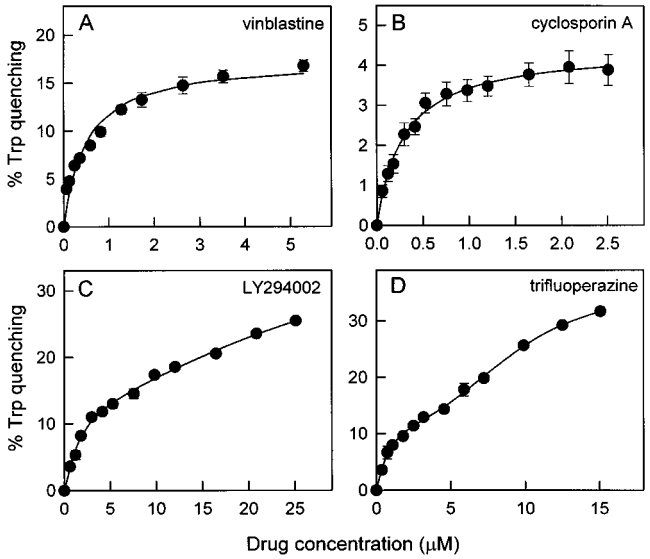

FIGURE 7: Effect of binding of various drugs and hydrophobic peptides on the intrinsic Trp fluorescence of Pgp. Increasing concentrations of (A) vinblastine, (B) cyclosporin A, (C) LY294002, and (D) trifluoperazine were added at 22 °C to a 100 μg/mL solution of purified Pgp in buffer containing 2 mM CHAPS and 0.5 mg/mL PMPC. Fluorescence emission at 330 nm was recorded at 22 °C following excitation at 290 nm. The quenching curve for cyclosporin A was essentially monophasic, and was fitted to an equation describing binding to a single type of site (indicated by the solid lines). Vinblastine quenching showed some biphasic character, and could be fitted to equations for either one or two sites; one-site fitting is shown here. For LY294002 and trifluoperazine, clearly biphasic quench curves were obtained, which were fitted to a model with two binding sites, one of high and one of low affinity (*32*). Where not visible, error bars are contained within the symbols.

can give quantitative estimates of binding affinity. Binding of the nonhydrolyzable analogue AMP-PNP gave similar results (Figure 6B), with a K_d of 0.21 mM. The change in Trp fluorescence appears to be brought about by nucleotide binding, rather than hydrolysis, since both hydrolyzable (ATP) and nonhydrolyzable molecules (ADP and AMP-PNP) gave similar values for ΔF_{max} of ~10%.

Binding of fluorescent TNP-nucleotides resulted in very strong quenching of Trp fluorescence (Figure 6C,D), with ΔF_{max} values approaching ~80% (Table 2). The estimated K_d values of 51 and 44 μM for TNP-ATP and TNP-ADP, respectively, agree well with values obtained previously by enhancement of TNP fluorescence following binding of the fluorescent nucleotides to Pgp (*37*).

Quenching of Trp Residues by Binding of Drug and Peptide Substrates. Addition of various drug and peptide substrates also resulted in saturable, concentration-dependent quenching of Trp fluorescence (Figure 7). Two different quenching patterns were observed. Some substrates, such as the cyclic peptide modulator cyclosporin A (Figure 7B), gave essentially monophasic quench curves that could be fitted to a single K_d value. Other drugs, such as the phosphoinositide-3-kinase inhibitor LY294002 (*38*) (Figure 7C) and the modulator trifluoperazine (Figure 7D), gave rise to clearly biphasic curves, which were fitted to a two-site model with high- and low-affinity binding sites. Biphasic curves have been observed previously for quenching of MIANS-labeled Pgp by several drugs, and were interpreted as indicating the existence of two different drug binding sites of differing

affinity (*39*). The quench curve for some drugs, such as vinblastine (Figure 7A), showed some biphasic character, and could be fitted to either a single value of K_d, or two values with affinities that were close to each other in magnitude. All of the linear and cyclic peptides tested gave monophasic quench curves, implying that they may only bind to a single site within Pgp, whereas many of the non-peptide drug substrates showed biphasic characteristics, suggesting multiple binding sites (Table 2).

The estimated values of K_d and ΔF_{max} (or ΔF_{max1} and ΔF_{max2} for biphasic plots) for many Pgp substrates in different structural classes are shown in Table 2. In general, the binding affinities obtained by quenching of Trp fluorescence are very similar to those estimated from quenching of the fluorescence of MIANS-Pgp (*6*, *7*). However, the use of Trp quenching has some additional advantages. Certain substrates are highly fluorescent in the same wavelength range as MIANS, making the estimation of K_d values using that method impossible. The phosphoinositide-3-kinase inhibitor LY294002 falls into the latter category. We have confirmed that this compound is in fact a Pgp substrate by independent functional experiments; it blocks colchicine transport by Pgp in vesicle systems and stimulates Pgp ATPase activity 4-fold at a concentration of 5−10 μM (P. Lu and F. J. Sharom, unpublished data).

The values of ΔF_{max} covered a wide range for different substrates, from 4 to 100%. Some compounds, notably the rhodamine dyes, produced very strong quenching, e.g., rhodamine 123 and rhodamine B (Table 2). In general, non-peptide drugs showed ΔF_{max} values of at least 15%. The hydrophobic peptide substrates and modulators, both linear and cyclic, all displayed relatively low maximal quenching, with ΔF_{max} values in the range 4−6%. The monophasic nature of the quenching and the low quenching efficiency by comparison with drug substrates suggest that peptides may interact with Pgp in a different region from the other non-peptide drugs.

Previous work in our laboratory has shown that ATP and drugs bind to MIANS-Pgp in a random order (*8*). However, MIANS-labeled protein is catalytically inactive, and is blocked from proceeding through the catalytic cycle following substrate binding. We therefore investigated the quenching of Trp residues in native catalytically active Pgp, following sequential titration with nucleotide and two different drugs, in either order. Figure 8A shows the results obtained by titration with vinblastine to saturation, followed by titration of TNP-ATP, whereas Figure 8B displays the data for the titration carried out in the reverse order. TNP-ATP can be hydrolyzed by Pgp, but at a lower rate than unmodified ATP (*37*). Following saturation with vinblastine, titration with TNP-ATP produces the same characteristically large saturable quenching observed for the nucleotide alone, with a K_d of 64 μM, similar to the value of 51 μM observed in the absence of drug. Thus, the affinity of nucleotide binding is changed only slightly by prior binding of vinblastine. When TNP-ATP is bound to Pgp first to give a large amount of quenching, subsequent titration with vinblastine gives a much smaller increase in quenching than is observed with drug alone. Similar results were seen for dual titrations of TNP-ATP and daunorubicin (Figure 8C,D). Titration with TNP-ATP following daunorubicin binding resulted in a large degree of quenching, with a K_d value of

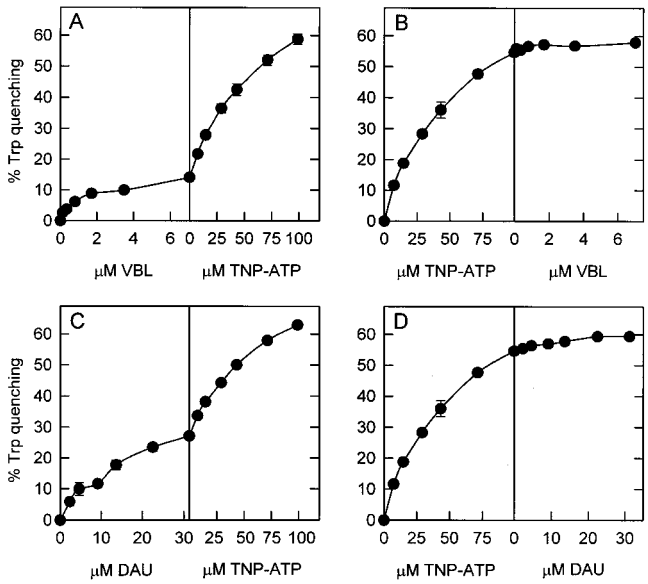

FIGURE 8: Quenching of the intrinsic Trp fluorescence of Pgp by sequential addition of nucleotides and drugs. In (A) and (B), increasing concentrations of vinblastine (VBL) and TNP-ATP were added sequentially, either vinblastine first (A) or TNP-ATP first (B), to a 100 μg/mL solution of purified Pgp in buffer containing 2 mM CHAPS and 0.5 mg/mL PMPC. Fluorescence emission at 330 nm was recorded at 22 °C following excitation at 290 nm. (C) and (D) show a similar series of experiments using sequential titration of daunomycin (DAU) and TNP-ATP. Where not visible, error bars are contained within the symbols.

65 μM, whereas if TNP-ATP was bound first, subsequent daunomycin binding gave a very small increase in quenching. For vinblastine and daunorubicin, the combination of drug and TNP-ATP resulted in ΔF_{max} values similar to those seen for TNP-ATP alone; i.e., quenching by substrate and nucleotide was not additive. These results suggest that a fixed maximal level of quenching is reached after binding of a combination of nucleotide and drug substrate.

Mechanism of Quenching by Nucleotides, Drugs, and Peptides. The mechanism of quenching of Pgp Trp residues by nucleotides, drugs, and hydrophobic peptides is of interest in that it may provide important insights into the relative locations of the different domains of the transporter. Since Pgp fluorescence is very highly quenched by TNP-ATP/ADP, a large fraction of the Trp residues contributing to fluorescence emission may be located close to the nucleotide binding site. Quenching could take place either by a direct interaction (static quenching) or by FRET, since there is substantial overlap between the emission spectrum of Trp and the absorption spectrum of TNP-ATP. FRET is expected to result in lower fluorescence lifetimes for the Trp residues (*31*). However, lifetime measurements showed essentially no change in Trp lifetimes following addition of a TNP-ATP concentration close to K_d (Table 3). Fluorescence lifetime measurements also showed no significant decrease in Trp lifetime following addition of a similar concentration of ATP and AMP-PNP (data not shown). Comparable results were obtained when Pgp was saturated with various drugs; in fact, the lifetime increased slightly in the presence of some compounds (Table 3). Combinations of AMP-PNP and various drugs and modulators also resulted in little change in fluorescence lifetime (data not shown). These results initially suggest that quenching by both nucleotides and drugs may take place by a static, direct binding mechanism.

Table 3: Trp Fluorescence Lifetimes in the Absence and Presence of Nucleotides and Drugs[a]

	α_1	τ_1 (ns)	α_2	τ_2 (ns)	$\langle\tau_{av}\rangle$ (ns)
Pgp alone	0.55	0.96	0.74	4.1	2.76
nucleotide binding					
50 μM TNP-ATP	0.69	1.0	0.42	4.0	2.14
drug binding					
10 μM vinblastine	1.07	1.1	0.51	4.4	2.17
40 μM daunorubicin	0.71	1.3	0.52	4.4	2.61
30 μM trifluoperazine	0.72	1.1	0.35	4.3	2.15
10 μM tetramethylrosamine	0.55	1.1	0.50	3.9	2.43
50 μM rhodamine 123	0.65	1.5	0.43	4.6	2.73
150 μM colchicine	0.66	1.4	0.39	4.7	2.63

[a] Two-exponential decay analysis was carried out; α is the preexponential value; τ is the fluorescence lifetime; $\langle\tau_{av}\rangle$ is the amplitude average lifetime.

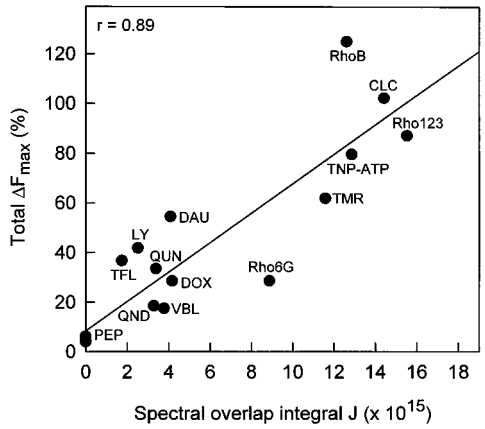

FIGURE 9: Relationship between the value of the maximal Trp quenching parameter, total ΔF_{max}, and the spectral overlap integral, *J*, for various Pgp substrates: trifluoperazine (TFL); LY294002 (LY); daunorubicin (DAU); doxorubicin (DOX); quinine (QUN); quinidine (QND); vinblastine (VBL); rhodamine 6G (Rho6G); tetramethylrosamine (TMR); rhodamine 123 (Rho123); TNP-ATP; colchicine (CLC); and the six peptide substrates listed in Table 2 (PEP).

However, given the high level of quenching observed for some nucleotides (e.g., TNP-ATP) and drugs (e.g., rhodamines B and 123), this would imply that all Trp residues contributing to fluorescence participate in direct binding of these substrates, which seems unreasonable. It seems more likely that some Trp residues are located not directly at the binding sites for nucleotides and drugs, but sufficiently close that they are well below the FRET distance, R_0. These residues would thus be completely quenched by energy transfer ($E = \sim 1$) following substrate binding, and the remaining fraction of unquenched Trps would give rise to the observed fluorescence intensity with an unchanged lifetime.

To further explore the possible relationship between quenching and FRET, we calculated the spectral overlap integral, *J*, for Trp and the various nucleotides and drugs. As shown in Figure 9, there is a good correlation ($r = 0.89$) between the value of total ΔF_{max} ($\Delta F_{max1} + \Delta F_{max2}$, see Table 2), as an indicator of quenching efficiency, and *J*. This suggests that for TNP-ATP and most drugs, energy transfer from Trp residues to the bound substrate is a major mechanism of the observed quenching. The high degree of quenching observed for both nucleotides and drug substrates suggests that they bind to a location within the protein that is close to the emitting Trp residues. It is interesting that compounds such as rhodamine 123, rhodamine B, and TNP-ATP, which contain aromatic rings, were the most efficient quenchers of Trp fluorescence. If quenching results from the localization of substrates close to Trp residues, it might be expected that interactions such as $\pi-\pi$ stacking would be more likely for aromatic substrates.

DISCUSSION

Based on a topology model (Figure 1) similar to that proposed for the murine mdr3 protein (*35*), the eight Trp residues in the N-half of hamster class I Pgp are located in the N-terminal tail (Trp44), in TM2, TM4, and TM5 (Trp133, Trp229, and Trp312, respectively), in the first cytoplasmic loop (Trp159), in the second extracellular loop (Trp209), and in the linker region immediately following NB1 (Trp695 and Trp705). The C-half of Pgp contains three Trp residues: Trp800 in cytoplasmic loop 3, Trp852 in extracellular loop5, and Trp1105 between the Walker A and B motifs of NB2. The intrinsic fluorescence spectrum of Pgp attributable to Trp residues indicates that all are located in a relatively nonpolar local environment. Acrylamide quenching experiments indicated a single class of Trps, all located in a very similar environment characterized by low accessibility to aqueous solvent. Thus, it appears that the Trp residues predominantly contributing to the fluorescence emission spectrum of Pgp may be located within hydrophobic or membrane-bound regions of the protein. The slope of the Stern-Volmer plot for quenching by acrylamide (2.6 M^{-1}) also suggests that the emitting Trp residues have low solvent accessibility. By comparison, the slopes of the Stern-Volmer plots for acrylamide quenching of the intrinsic Trp fluorescence of the plasma membrane and SERCA1 Ca^{2+}-ATPases were 2.9 and 1.9 M^{-1}, respectively(*11, 12*). The Trp residues in both of these proteins are mostly contained within the membrane-spanning domains. Quenching with I^- also indicated that the Trps of Pgp are poorly accessible to quencher, and suggested the existence of two classes of residues, one of which was highly inaccessible to this reagent, and thus largely buried. Our I^- quenching results differ from those of Sonveaux et al. (*21*), who reported a linear Stern-Volmer plot, with a high degree of quenching in the presence of ATP, more typical of a denatured protein [for more discussion of this point, see (*6*)]. The fluorescence lifetime data for Pgp Trps in the presence of acrylamide were complex, with a less than expected decrease in lifetime and a shift in the values of the preexponential factors, suggesting the existence of a static quenching component. Similar observations were made by Eftink and Wasylewski for the single Trp protein cod parvalbumin (*40*). They concluded that for proteins showing this type of behavior, an analysis based on a continuous distribution of lifetimes and dynamic quenching constants, or a more complex discrete fitting model based on three lifetime components, may be necessary.

The only Trp residue for which independent fluorescence information is available to date is Trp1106 of the mouse mdr3 protein (equivalent to hamster Trp1105) located within NB2, which was expressed as a separate domain (*25*). It exhibited an emission maximum at 328 nm, indicating a hydrophobic environment. Thus, the three Trps in TM helices, plus Trp1105, would be expected to display spectra characteristic of a nonpolar environment. Nothing is known about the polarity of the local environment surrounding the Trps in short extracellular loops (Trp209 and -852) or in cytoplasmic

regions (Trp44, -159, -695, -705, and -800), where folding into small domains may be possible. However, it seems reasonable to assume that at least some of these residues would be located in a polar environment accessible to solvent. The fact that this is not observed experimentally suggests that these residues may be quenched. Two common quenchers of Trp fluorescence are water and peptide bonds, as well as several amino acid side chains. Chen and Barkley recently identified the amino acid side chains that can quench Trp fluorescence in proteins (*41*); they include Gln, Asn, Glu, Asp, Cys, and His (which quench by excited-state electron transfer) as well as Lys and Tyr (which quench by excited-state proton transfer). Thus, several of the Trp residues in Pgp might well be quenched by one or more of these mechanisms. The fact that the quantum yield of the Trp residues in Pgp was low (0.03) also suggests the existence of internal quenching.

The lifetime of Trp residues in proteins varies from a few hundred picoseconds to 9 ns. Lifetime measurements of purified Pgp indicated the presence of two components: one with a shorter lifetime (0.6−1 ns), and the other major component with a longer lifetime of ∼4 ns. It is tempting to speculate that these might represent two classes to Trps: those buried deeply in TM domains and those in more accessible regions. However, in a number of studies, even single Trp proteins (*42*) and the Trp monomer (*43*−*45*) have been observed to show multiple lifetime components, making the time-resolved data difficult to interpret in terms of individual residues. Further experiments are needed to shed more light on the origin of the two lifetime components of Trp-rich Pgp. In this regard, the ability to examine the behavior of single-Trp Pgp mutants would be of immense advantage. The stage has been set for production of these types of engineered proteins with the recent report of the construction of a partially functional Trp-less Pgp (*46*).

To investigate possible conformational changes taking place on binding of substrates, we carried out acrylamide quenching studies in the presence of nucleotides, drugs, and combinations of the two. Only very small changes in the slopes of the Stern-Volmer plots were noted following saturation with any of these molecules, arguing against major conformational changes that alter the environment of Trp residues following substrate binding. These results support our previous observations that a MIANS label within the catalytic sites of Pgp is only slightly less accessible to solvent (K_{SV} was reduced by ∼10%) when the nucleotide binding sites are occupied (*37*), suggesting that the conformational change induced by nucleotide binding is small. In contrast, it was recently reported that the slope of the Stern-Volmer plot for acrylamide quenching of purified Pgp was substantially altered following nucleotide and drug binding (*22*). However, this study looked at only a very narrow range of acrylamide concentrations (0−0.08 M), and the fluorescence changes observed were only a maximum of 4−10% at the highest concentration. Moreover, under some conditions, no acrylamide quenching at all was noted (the slope of the Stern-Volmer plot was zero, a very unusual observation), suggesting that caution should be observed when interpreting these data.

Pgp Trp residues were quenched in a saturable fashion by binding of various nucleotides, both hydrolyzable (ATP) and nonhydrolyzable (ADP, AMP-PNP). Since all gave similar changes in fluorescence (ΔF_{max} of ∼10%), the change in Trp fluorescence appears to be brought about by nucleotide binding, rather than hydrolysis. The K_d values estimated from fitting the data to an equation describing binding to a single type of site were in the range 0.2−0.3 mM, in good agreement with values obtained from MIANS-Pgp quenching (*7*, *8*), and close to the K_M for ATP hydrolysis (*27*). The fluorescent nucleotide analogues TNP-ATP and TNP-ADP caused highly efficient quenching of the Pgp fluorescence, with ΔF_{max} values approaching 80%. Again, saturable titration of these nucleotide analogues gave K_d values in good agreement with determinations made by other methods (*37*). Binding of several fluorescent nucleotides (including TNP-ATP) to the helicase DnaB also results in strong quenching of the Trp fluorescence (*13*). It was shown that in this case quenching arises from highly efficient energy transfer to the fluorescent derivative from Trp residues, which are clustered together near the nucleotide binding sites. As discussed below, it seems likely that the quenching of Pgp Trp fluorescence by TNP-nucleotides also arises from FRET.

Pgp Trp residues were also highly sensitive to binding of substrates, with various drugs, modulators, and hydrophobic peptides causing saturable concentration-dependent quenching of the fluorescence. Trp quenching by some substrates displayed biphasic characteristics, suggesting the existence of two drug binding sites with different affinities. We previously reported similar results for binding of three drugs to MIANS-labeled Pgp reconstituted into lipid bilayers (*39*). Sequential titration with both drug and nucleotide confirmed our previous observations (made with catalytically inactive MIANS-Pgp) that binding of these substrates can take place in any order (*8*). The observation that quenching caused by TNP-ATP and vinblastine was not additive suggests that a maximal level of quenching is reached in the loaded transporter, perhaps reflecting the attainment of a transport-competent conformation.

The presence of phospholipid proved necessary for observation of nucleotide and drug-induced quenching of Trp fluorescence, suggesting that it plays an important modulatory role in substrate binding. However, the addition of lipid did not produce a significant change in the Trp emission maximum or fluorescence lifetimes. We previously reported that quenching of MIANS-labeled Pgp by substrates also required the presence of phospholipids (*8*), and more recently, we showed that the apparent affinity of drug binding depends on the lipid environment (*39*). Lipids may be necessary for maintaining Pgp conformation, as well as providing a "pool" into which drugs can partition to access the transporter binding site(s), which appear to lie within the membrane-spanning regions of the protein [for a review, see (*47*)].

There are several precedents for complete quenching of Trps in a membrane transporter by binding of drugs. Saturable binding of the volatile anesthetic halothane to the plasma membrane Ca^{2+}-ATPase also results in saturable quenching of >80% of the Trp fluorescence (ΔF_{max} approaches 100%) (*11*). This protein contains 11 Trp residues, which do not appear to be solvent accessible, based on fluorescence studies. Quenching in this case was not due to energy transfer, but was speculated to arise from either a direct interaction of the Br atom in halothane with Trp residues in the protein, or possibly a conformational change.

The existence of a good correlation between the maximal degree of quenching, ΔF_{max}, and the spectral overlap integral, *J*, indicated that for most drugs, energy transfer from the Trp residues to the bound substrate is the most likely mechanism of quenching. The very small measured changes in fluorescence lifetime (Table 3) suggested that some Trp residues are located close to the bound drug, so that highly efficient energy transfer takes place, resulting in complete quenching. The remaining fluorescence emission would then arise from unquenched Trps with an unchanged lifetime. The relatively high level of quenching observed for many drugs implies that the Trps contributing to Pgp intrinsic fluorescence are located relatively close to the drug binding sites. Since these residues are probably largely membrane-bound, based on their fluorescence emission maximum and their quenching properties, this conclusion is consistent with the idea that drug binding takes place within the membrane-spanning regions of Pgp.

Table 2 shows a wide range of values for total ΔF_{max} (which reflects the quenching efficiency), ranging from 4−6% for hydrophobic peptides to essentially complete quenching for some of the rhodamine dyes and colchicine. If quenching results primarily from FRET following binding of drug close to Trp residues, then the magnitude of total ΔF_{max} will reflect both the intrinsic properties of the drug itself (i.e., its chemical makeup, *J* value) as well as its proximity to the Trp residues. The presence of multiple drug binding sites, each of which would likely have somewhat different distance relationships with the Trp residues, will have an effect on FRET (and thus quenching) efficiency, accounting for some of the scatter in Figure 9.

It is possible that drugs could quench Pgp Trp residues by an indirect mechanism. For example a relatively large conformational change taking place in the membrane-spanning regions of Pgp induced by drug binding might move chemical groups within the protein to positions where they could efficiently quench Trp residues. Such a change seems unlikely, given the very small changes in Trp susceptibility to acrylamide quenching that were noted following binding of three different substrates (Figure 4).

Quenching of Trp fluorescence is also observed for nucleotides, raising the question of the mechanism by which this takes place. In the case of unmodified molecules such as ATP, ADP, and AMP-PNP, the maximal quenching, although relatively low (in the 10% range), is larger than that of linear and cyclic peptide substrates, and only slightly smaller than that of vinblastine and quinidine. Acrylamide quenching studies using MIANS-Pgp have already suggested that only small changes in the conformation of the NB domains take place on nucleotide binding (*37*). In addition, binding of either ATP or AMP-PMP to Pgp in this study resulted in insignificant changes in Trp accessibility to acrylamide (Figure 4), which suggests that nucleotide-induced conformational changes in the membrane-bound domains of Pgp affecting the Trp residues are also very small. Since a large conformational change is improbable, it seems likely that the Trp quenching observed for ATP and ADP also arises from FRET, which would imply that the site for nucleotide binding is close to the membrane-bound Trp residues, and by extension, close to the drug binding sites. This proposal is supported by the very strong Trp quenching ($\Delta F_{max} \sim 80\%$, see Table 2) observed for TNP-nucleotides. Since ATP and TNP-ATP bind competitively to the same site on Pgp (*37*), the high *J* value of the TNP group presumably accounts for the high level of quenching observed with the modified nucleotide. The separately expressed C-terminal NB domain of Pgp contains a single Trp residue, which has been shown to "report" nucleotide binding by quenching. However, ∼80% quenching of the intrinsic fluorescence of full-length Pgp containing 11 Trp residues cannot be accounted for by the proximity of a single residue to the bound nucleotide. Taken together, our results strongly suggest that both the drug and ATP binding sites of Pgp are located in close proximity to each other, and to the membrane-bound Trp residues, indicating that the regions of the molecule involved in binding and transport may be packed together quite compactly. Such proximity between the two types of binding sites would facilitate coupling between drug transport and ATP hydrolysis.

ACKNOWLEDGMENT

We extend our thanks to Photon Technology International Canada Inc. of London, Ontario, for generously making the fluorescence lifetime facilities in their Fast Kinetics Application Laboratory available to us.

REFERENCES

1. Holland, I. B., and Blight, M. A. (1999) *J. Mol. Biol. 293*, 381−399.
2. Doige, C. A., and Ames, G. F. (1993) *Annu. Rev. Microbiol. 47*, 291−319.
3. Schinkel, A. H. (1999) *Adv. Drug Deliv. Rev. 36*, 179−194.
4. Chan, H. S., Grogan, T. M., DeBoer, G., Haddad, G., Gallie, B. L., and Ling, V. (1996) *Eur. J. Cancer 32A*, 1051−1061.
5. Bradshaw, D. M., and Arceci, R. J. (1998) *J. Clin. Oncol. 16*, 3674−3690.
6. Sharom, F. J., Liu, R. H., and Romsicki, Y. (1998) *Biochem. Cell Biol. 76*, 695−708.
7. Sharom, F. J., Liu, R. H., Romsicki, Y., and Lu, P. H. (1999) *Biochim. Biophys. Acta 1461*, 327−345.
8. Liu, R., and Sharom, F. J. (1996) *Biochemistry 35*, 11865−11873.
9. Sharom, F. J., Lu, P., Liu, R., and Yu, X. (1998) *Biochem. J. 333*, 621−630.
10. Weber, J., Wilke-Mounts, S., Hammond, S. T., and Senior, A. E. (1998) *Biochemistry 37*, 12042−12050.
11. Lopez, M. M., and Kosk-Kosicka, D. (1998) *Biophys. J. 74*, 974−980.
12. Gryczynski, I., Wiczk, W., Inesi, G., Squier, T., and Lakowicz, J. R. (1989) *Biochemistry 28*, 3490−3498.
13. Bujalowski, W., and Klonowska, M. M. (1994) *J. Biol. Chem. 269*, 31359−31371.
14. Guixe, V., Rodriguez, P. H., and Babul, J. (1998) *Biochemistry 37*, 13269−13275.
15. Mus-Veteau, I., Pourcher, T., and Leblanc, G. (1995) *Biochemistry 34*, 6775−6783.
16. Weitzman, C., Consler, T. G., and Kaback, H. R. (1995) *Protein Sci. 4*, 2310−2318.
17. Pawagi, A. B., Wang, J., Silverman, M., Reithmeier, R. A., and Deber, C. M. (1994) *J. Mol. Biol. 235*, 554−564.
18. Zheleznova, E. E., Markham, P., Edgar, R., Bibi, E., Neyfakh, A. A., and Brennan, R. G. (2000) *Trends Biochem. Sci. 25*, 39−43.
19. Zheleznova, E. E., Markham, P. N., Neyfakh, A. A., and Brennan, R. G. (1999) *Cell 96*, 353−362.
20. Popkov, M., Lussier, I., Medvedkine, V., Estève, P. O., Alakhov, V., and Mandeville, R. (1998) *Eur. J. Biochem. 251*, 155−163.

21. Sonveaux, N., Shapiro, A. B., Goormaghtigh, E., Ling, V., and Ruysschaert, J. M. (1996) *J. Biol. Chem. 271*, 24617−24624.
22. Sonveaux, N., Vigano, C., Shapiro, A. B., Ling, V., and Ruysschaert, J. M. (1999) *J. Biol. Chem. 274*, 17649−17654.
23. Baubichon-Cortay, H., Baggetto, L. G., Dayan, G., and Di Pietro, A. (1994) *J. Biol. Chem. 269*, 22983−22989.
24. Dayan, G., Baubichon-Cortay, H., Jault, J. M., Cortay, J. C., Deleage, G., and Di Pietro, A. (1996) *J. Biol. Chem. 271*, 11652−11658.
25. Conseil, G., Baubichon-Cortay, H., Dayan, G., Jault, J. M., Barron, D., and Di Pietro, A. (1998) *Proc. Natl. Acad. Sci. U.S.A. 95*, 9831−9836.
26. Sharom, F. J., Yu, X., Lu, P., Liu, R., Chu, J. W., Szabo, K., Muller, M., Hose, C. D., Monks, A., Varadi, A., Seprodi, J., and Sarkadi, B. (1999) *Biochem. Pharmacol. 58*, 571−586.
27. Sharom, F. J., Yu, X., Chu, J. W. K., and Doige, C. A. (1995) *Biochem. J. 308*, 381−390.
28. Groenzin, H., and Mullins, O. C. (2000) *J. Phys. Chem. A 103*, 11237−11245.
29. James, D. R., Siemiarczuk, A., and Ware, W. R. (1992) *Rev. Sci. Instrum. 63*, 1710−1716.
30. Siemiarczuk, A., Wagner, B. D., and Ware, W. R. (1990) *J. Phys. Chem. 94*, 1661−1666.
31. Lakowicz, J. R. (1999) in *Principles of Fluorescence Spectroscopy*, Kluwer Academic Publishers, New York.
32. Doppenschmitt, S., Spahn-Langguth, H., Regardh, C. G., and Langguth, P. (1998) *Pharm. Res. 15*, 1001−1006.
33. Eftink, M. R. (1991) in *Methods of Biochemical Analysis, Volume 35: Protein Structure Determination* (Suelter, C. H., Ed.) pp 127−205, John Wiley, New York.
34. Devine, S. E., and Melera, P. W. (1994) *Cancer Chemother. Pharmacol. 33*, 465−471.
35. Kast, C., Canfield, V., Levenson, R., and Gros, P. (1996) *J. Biol. Chem. 271*, 9240−9248.
36. Romsicki, Y., and Sharom, F. J. (1998) *Eur. J. Biochem. 256*, 170−178.
37. Liu, R., and Sharom, F. J. (1997) *Biochemistry 36*, 2836−2843.
38. Vlahos, C. J., Matter, W. F., Hui, K. Y., and Brown, R. F. (1994) *J. Biol. Chem. 269*, 5241−5248.
39. Romsicki, Y., and Sharom, F. J. (1999) *Biochemistry 38*, 6887−6896.
40. Eftink, M. R., and Wasylewski, Z. (1989) *Biochemistry 28*, 382−391.
41. Chen, Y., and Barkley, M. D. (1998) *Biochemistry 37*, 9976−9982.
42. Vincent, M., Brochon, J. C., Merola, F., Jordi, W., and Gallay, J. (1988) *Biochemistry 27*, 8752−8761.
43. James, D. R., and Ware, W. R. (1985) *Chem. Phys. Lett. 120*, 450−454.
44. Szabo, A. G., and Rayner, D. M. (1980) *J. Am. Chem. Soc. 102*, 554−563.
45. Chang, M. C., Petrich, J. W., McDonald, D. B., and Fleming, G. R. (1983) *J. Am. Chem. Soc. 105*, 3819−3824.
46. Kwan, T., Loughrey, H., Brault, M., Gruenheid, S., Urbatsch, I. L., Senior, A. E., and Gros, P. (2000) *Mol. Pharmacol. 58*, 37−47.
47. Loo, T. W., and Clarke, D. M. (1999) *Biochim. Biophys. Acta 1461*, 315−325.

BI0018786